American Journal of Environmental Sciences

Research Article

Development and Validation of a 2D Finite Element Model for Air Pollution Dispersion (SUITE-2D)

Youssef Ismail Hafez

Private Consultant and Former Professor at Nile Research Institute, Delta Barrage, El Qanater, Greater Cairo, Egypt

Article history
Received: 08-04-2025
Revised: 03-07-2025
Accepted: 04-10-2025

Email:
youssefhafez995@gmail.com

Abstract: This paper presents the development and validation of SUITE-2D (Solving Unsteady Incompressible Transport Equation in Two Dimensions), a two-dimensional finite element model for solving the advection-diffusion transport equation with decay and source terms. The model provides an efficient and accurate approach for simulating pollutant dispersion in environmental systems. The finite element formulation uses the standard Galerkin method, with numerical integration performed using Gaussian quadrature. Time integration schemes such as central, backward, and forward differences are incorporated for flexibility. SUITE-2D is validated against exact analytical solutions of unsteady advection-diffusion problems, yielding low relative errors and demonstrating computational efficiency. This means that the study focuses on rigorous mathematical validation of SUITE-2D using exact analytical solutions. Real-world datasets are not used, as field measurements often contain uncertainties that hinder true validation of numerical solvers. Instead, such solvers, once validated, are used to interpret or verify observed field patterns, highlighting the model's potential for environmental impact assessments and regulatory decision-making. Comparisons with the SUITE-3D model reveal the computational advantages and limitations of two-dimensional modeling for air pollution scenarios.

Keywords: Advection-Diffusion Equation, Finite Element Method (FEM), Air Pollution Modeling, Two-Dimensional Modeling, SUITE-2D Model, Numerical Validation

Introduction

Transport phenomena play a fundamental role in various environmental engineering phenomena, applied mathematics, and scientific fields. Understanding the movement of mass and heat in various media, such as solids, fluids, and gases, is essential for addressing challenges like air pollution, water and soil pollution, heat transfer, and hydrodynamic flows. Air pollution is created from the activities of industrial enterprises, power plants, and cars, which emit hundreds of tons of harmful substances into the atmosphere. Photochemical processes constantly occur in the air basin, leading to the emergence of new compounds, sometimes more harmful than the initial ones (Issakhov *et al*., 2020). With the rapid advancement of urbanization and industrialization in cities, air pollution has become one of the significant environmental challenges and issues in many countries. The concentration of particulate matter with an aerodynamic diameter of less than 2.5 μm (PM 2.5), recognized as the main air pollutant in Iran, penetrates the respiratory system through inhalation, causing respiratory and cardiovascular diseases, reproductive disorders, central nervous system disturbances, and cancer. Accurate and high spatiotemporal modeling of air pollutant concentrations is crucial for air quality management and exposure assessment in epidemiological studies (Sohrabi and Maleki, 2025).

The simplest dispersion models are steady-state Gaussian plume models. They are based on mathematical approximation of the plume behaviour and follow some basic assumptions that may not always present a realistic scenario. More recently, advanced dispersion models are being developed, which are based on a more refined approach of simulating the dispersion phenomenon following the properties of the atmosphere rather than

relying on general mathematical approximations. This has expanded the field of modelling to tackle difficult situations such as complex terrain and long-distance transport. (Khan and Hassan, 2021; Leelossy *et al*., 2014; Daly and Zannetti, 2007). Enciso-Díaz *et al.* (2025) conducted a review to analyze global trends in the use of air pollution models under the influence of Climate Variability (CV) over urban areas. They found that Temperature emerged as the dominant climate variable, followed by wind, precipitation, humidity, and solar radiation.

Mathematical models based on the Advection-Diffusion (AD) equation provide a robust framework for analyzing these processes (Al-khafaji and Al-Zubaidi, 2025). Advancements in computational power have further enabled the development of sophisticated numerical models to simulate these transport mechanisms accurately (e.g., Cheng and Zheng, 2020; Saqib *et al*., 2017; Hafez, 2022a). Recent advancements in numerical modeling have enabled high-resolution simulations of pollutant dispersion in complex environments, such as urban canyons, using Finite Element Methods (FEM) and hybrid modeling approaches.

Air pollution, particularly the dispersion of pollutants from industrial sources, remains a pressing environmental concern in the context of climate change and global warming. While established models like CALPUFF and AERMOD remain widely used in industrial impact assessments, recent studies highlight discrepancies in performance under low-wind or complex terrain conditions. Accurate modeling of pollutant dispersion is crucial for developing environmental management strategies and obtaining regulatory permits for industrial activities. The complexity of modeling air pollution arises from the dynamic nature of atmospheric conditions and the spatial variability of pollutant transport (Cheng and Zheng, 2020).

The advection-diffusion transport equation has been extensively studied across different dimensional scales. One-Dimensional (1D) models (e.g., Hafez and Awad, 2016; Putri *et al*., 2018; Hafez, 2022b; Al-khafaji and Al-Zubaidi, 2025) simplify the analysis by assuming uniformity along certain planes but are limited in capturing spatial variations. On the other hand, three-dimensional (3D) models (e.g., Cheng and Zheng, 2020; Saqib *et al*., 2017; Hafez, 2022a) provide comprehensive insights but are computationally expensive. Two-Dimensional (2D) models strike a balance between computational efficiency and representational accuracy by allowing variations in two spatial dimensions (e.g., Svoboda, 2000; Talaa *et al*., 2002; Jha *et al*., 2013).

This study focuses on rigorous mathematical validation of SUITE-2D using exact analytical solutions. Real-world datasets are not used, as field measurements often contain uncertainties that hinder true validation of numerical solvers. Instead, such solvers, once validated, are used to interpret or verify observed field patterns. In other words, this study emphasizes mathematical and numerical validation of SUITE-2D to isolate and rigorously test each transport mechanism (advection, diffusion, decay). Field data are often inconsistent, limited in spatial/temporal resolution, or affected by external variability (wind shear, terrain), which can obscure model accuracy evaluations. Our position is that analytical solutions serve as the gold standard for validation of transport equations, a view shared by prior foundational works (Hafez, 2022a). Future extensions of SUITE-2D will focus on field-based case studies. The paper introduces the development and validation of SUITE-2D, a finite element model designed to solve the unsteady AD equation with decay and source terms. This model builds upon SUITE-3D (Hafez, 2022a), which demonstrated accurate pollutant dispersion under three-dimensional flow. SUITE-2D extends this work by offering a more efficient two-dimensional solver. While SUITE-3D highlighted the significance of including all three spatial dimensions in modeling air pollutant dispersion, it also revealed the computational challenges associated with 3D modeling. By focusing on two-dimensional transport, SUITE-2D aims to provide a more computationally efficient tool while maintaining accuracy for a wide range of environmental applications. SUITE-2D, developed herein, targets domains where vertical variation is minimal or can be approximated. It reduces computational costs significantly compared to SUITE-3D, which requires 5-10 times more runtime and memory.

The finite element approach adopted in SUITE-2D uses the standard Galerkin method, with central or implicit differencing in time ensuring numerical stability and accuracy. Gaussian quadrature is employed for numerical integration, and time integration schemes such as central, backward, and forward differences are incorporated for flexibility. Validation of SUITE-2D is conducted through comparisons with exact analytical solutions, demonstrating its high accuracy and computational efficiency.

In this study, SUITE-2D is applied to simulate air pollution dispersion scenarios, where it proves to be a valuable tool for environmental impact assessments. Comparisons with SUITE-3D are made to highlight the computational advantages and limitations of 2D modelling in practical applications. The results underscore the potential of SUITE-2D for providing insightful predictions while reducing computational costs.

Materials and Methods

Governing Equation and Finite Element Numerical Modelling

Several recent studies have explored the implementation of advection-diffusion solvers for reactive transport under varying environmental conditions, underscoring the need for accurate spatial and temporal resolution in dispersion modeling. Comparisons between Gaussian plume models

and full Eulerian solvers have shown that while the former are computationally efficient, the latter offer superior accuracy in transient and non-uniform conditions. The transport equation of an air pollutant is governed by the diffusion-advection differential equation. In three dimensions, it is expressed as:

$$\frac{\partial c}{\partial t} = D_x \frac{\partial^2 c}{\partial x^2} + D_y \frac{\partial^2 c}{\partial y^2} + D_z \frac{\partial^2 c}{\partial z^2} - u \frac{\partial c}{\partial x} - v \frac{\partial c}{\partial y} - w \frac{\partial c}{\partial z} - k\,c + R - S \quad (1)$$

Where c is the concentration, c (x, y, z, t) by mass (kg/m^3) of the air pollutant at location (x, y, z), x is the longitudinal coordinate (m), y is the lateral coordinate (m), and z is the vertical coordinate (m), t is time (s), D_x, D_y and D_z (m^2/s) are the diffusion coefficients in the x, y, and z directions respectively, u, v, and w (m/s) are the wind velocities in the x, y, and z directions respectively. In the context of air pollution, in Eq. (1), k is the substance decay coefficient (1/s), R is the source term due to aerial production (kg/m^3/s), and S is the sink term due to deposition (kg/m^3/s), Hafez (2022a). When two-dimensional analysis is applied, the domain can be either the horizontal plane (x and y) or the vertical plane (x and z) according to the problem at hand.

The governing equation is solved herein numerically by the Finite Element (FE) method. The details of using the finite element method to solve differential equations can be found in Molinas and Hafez (2000), Talaa *et al*. (2002), and Hafez (2017). In the finite element formulations, the governing equation is written in its weak form. That is, the weighted average of the governing differential equation over the domain of analysis is required to be zero for an arbitrary weighting function. This ensures that the approximation error or the residual is perpendicular (or orthogonal) to the Finite Element approximation functions. Consequently, the finite element approximation functions offer the minimum residual condition which is superior to either of the Finite Volume and Finite Difference Methods. Following the Galerkin method, the weighting function is interpreted as variation in the dependent variable.

In order to approximate the unknown function (required solution) for two-dimensional problems, the 4-node rectangular elements are used, which proved to be successful in Molinas and Hafez (2000); Talaa *et al*. (2002). The velocities in Eq. (1) are assumed constant within each element in order to eliminate possible errors in velocity determination on the transport of pollutants. However, velocities can be made variable and determined from a CFD model. Substitution of the finite element approximating function into the governing equation results in an integral equation. This equation is integrated over each element using four-point Gaussian quadrature. The contributions of all element integrations are added together to obtain a global matrix, the solution of which, after applying the appropriate boundary conditions, represents the finite element approximation of the differential equation, Eq. (1).

The mesh generation involved discretizing the computational domain into 4-node rectangular elements, with mesh densities carefully selected based on the requirements of the test case. The boundary conditions applied included both Dirichlet and Neumann types, with appropriate treatments along the domain edges and specific condition mapping tailored to each scenario. The initial conditions were defined by uniform concentration distributions across the domain at the start of the simulation. For time discretization, fixed time steps were employed, typically set to Δt = 1 second in the analytical case and 60 seconds for the point source pollution case. The solver settings utilized a central difference scheme for spatial discretization and an implicit method for time integration to ensure stability. Regarding convergence behavior, the model consistently achieved convergence within 1800 time steps, maintaining a relative error of less than 0.1%.

Several researchers applied their numerical solution methods to Eq. (1) by considering prototype cases, i.e., actual cases of air pollutants due to emission, for example, from industrial sources such as in Oyjinda and Pochai (2017; Oyjinda and Pochai, 2019). In these studies, no verifications of the proposed finite difference code were made either against analytical solutions or field data. In other situations, such as in Molinas and Hafez (2000); Talaa *et al*. (2002), comparison of the numerical model results was made against laboratory or field data without testing the numerical code with analytical solutions.

In this study testing of the developed numerical finite element code is made using analytical solutions that exist for two dimensional cases. By doing this, several advantages are gained, which include:

1) Making sure that the transport mechanisms, such as diffusion or advection, are modelled properly
2) Understanding the effect of each mechanism and how the different mechanisms interact with each other
3) Understanding the role of the boundary conditions of the problem at hand
4) Understanding the limits of the numerical modelling process through the investigation of changes in the model parameters

In the following, testing is made of each mechanism of the transport differential equation, and with the different combinations that are most likely to occur.

Results

Testing the Unsteady Diffusion Mechanism

Considering only the unsteady diffusion mechanism in a horizontal plane (x, y) yields the following transport equation:

DOI: 10.3844/ajessp.2025.89.109

$$\frac{\partial c}{\partial t} = D_x \frac{\partial^2 c}{\partial x^2} + D_y \frac{\partial^2 c}{\partial y^2} \quad (2)$$

Equation (2) contains two diffusion transport mechanisms in the *x* and *y* directions, respectively. As numerical errors in one direction might cancel the errors in the other direction giving a masking or cancellation effect, the equation is tested separately in each direction.

Case A

Choosing first the diffusion in the *x* direction simplifies Eq. (2) to:

$$\frac{\partial c}{\partial t} = D_x \frac{\partial^2 c}{\partial x^2} \quad (3)$$

For a length in the x direction equal to L, Eq. (3) has the following analytical solution, Edwards and Penney (2009):

$$c(x,t) = \sum_{n=1}^{\infty} b_n \exp(-n^2\ \pi^2\ D_x\ t/L^2) \sin(\frac{n\,\pi\,x}{L}) \quad (4)$$

Where the coefficients b_n are given by $b_n = \frac{2}{L}\int_0^L c(x,0)\sin\left(\frac{n\,\pi\,x}{L}\right)dx$, and $c(x,0)$ is the initial data function (here it represents the initial concentration) at time zero.

Figure (1) shows a hypothetical square domain with a side length equal to 50 m divided into 50 divisions in both the x and y directions. This yields 2500 four-node elements, resulting in each square element having a side length equal to 1 m. The central difference scheme is used to treat the time derivative, while the time step is taken equal to 1 second. The diffusion coefficient, D_x, is assumed equal to 0.15m^2/s. The boundary conditions include zero concentrations (c = 0) at x = 0 and x = 50 m, while zero normal gradients or fluxes (c_y = 0) are taken for the boundaries at y = 0 and y = 50 m, which represent isolating boundaries.

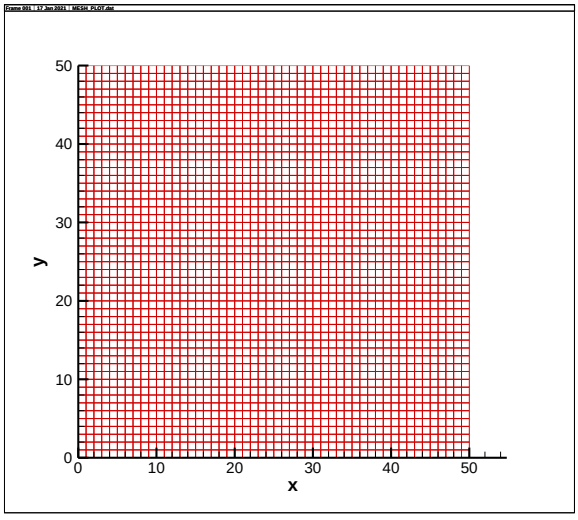

Fig. 1: Mesh of square domain with 50 m by 50 m divided into 2500 elements (50 by 50) for testing the unsteady diffusion in cases A, B, and C

The initial concentration distribution, $c(x, y, 0)$, is assumed to be constant, equal to 100 kg/m^3, which resembles a case of a uniform pollutant source along the whole domain with no wind velocities. This could also be a case of fire smoke emanating along the whole domain. The above conditions result in the following analytical solution:

$$c(x,t) = \frac{4*(100.0)}{\pi}\sum_{n=odd}^{\infty} \exp(-n^2\ \pi^2\ D_x\ t/L^2) \sin(\frac{n\,\pi\,x}{L}) \quad (5)$$

A total of 25 terms were found sufficient for calculating the Fourier series terms of the analytical solution appearing in Eq. (5). It is noted in Eq. (5) that the analytical solution does not include the y coordinates and this y coordinate independence indicates that the solution is the same along lines parallel to the x-axis.

Figure (2) shows a comparison between the Finite Element numerical solution and the analytical solution as given by Eq. (5) at any line parallel to the x-axis and at different times up to 1800 s (30 minutes), which requires 1800 time steps. The two numerical and analytical profiles are in excellent agreement with a maximum difference of the percentage relative error as small as 0.07%. The predicted concentration at the middle of the domain and at a time of 30 minutes, i.e., c (25, 25 m, 1800s) was found to be 43.81926 kg/m3, while the value given by the analytical solution is 43.84898 kg/m3, as seen in Table 1. This excellent match after 1800 time steps indicates that the FE numerical model is very accurate and stable, and no growth of round-off error occurs. Edwards and Penney (2009) found in their calculation of the concentration from Eq. (4), c (25 m, 1800s), that it is nearly 43.85. This value nearly coincides with the numerical model result.

Due to the insulation conditions at the ends y = 0 and y = 50 m, it is seen how the initial data as a horizontal plateau decreases toward the two ends at x = 0 and x = 50 m, and the concentration diffuses or escapes in lines parallel to the x-axis in a near parabolic shape. This resembles the diffusion of pollutants in Gauss plume models in the crosswind and vertical directions (y and z directions), where diffusion is the only mechanism assumed by these models. Table 1 shows a nonlinear decrease in the concentration with time at the middle of the domain at (x, y) = (25.0, 25.0), and an excellent match occurs between the numerical and analytical values with time. Figure (3) shows the concentration profile all over the square domain (Three Dimensional plot) at a time equal to 15 minutes, where the two insulated ends at y = 0 and y = 50 m cause the solution to be curved lines parallel to the x-axis. Figure (4) shows the profile at a time equal to 30 minutes, where further decrease of the concentration values (or diffusion out of the domain) occurs till the concentration becomes zero at all points at infinite time.

DOI: 10.3844/ajessp.2025.89.109

Table 1: Results of the SUITE-2D model versus analytical solutions

Time (s)	Case A X and Y coordinates (m, m)	Cases A and B FE Solution	Cases A and B Analytical Solution	Case C X and Y coordinates (m, m)	Case C FE Solution	Case C Analytical Solution
300	(25.0, 25.0)	98.33023	98.3184	(25.0, 50.0)	98.33021	98.31837
600	(25.0, 25.0)	87.49991	87.51852	(25.0, 50.0)	87.46700	87.48457
900	(25.0, 25.0)	74.33998	74.37169	(25.0, 50.0)	73.99393	74.02317
1200	(25.0, 25.0)	62.45531	62.48898	(25.0, 50.0)	61.40690	61.43816
1500	(25.0, 25.0)	52.33066	52.36282	(25.0, 50.0)	50.30396	50.33425
1800	(25.0, 25.0)	43.81926	43.84898	(25.0, 50.0)	41.06485	41.09312

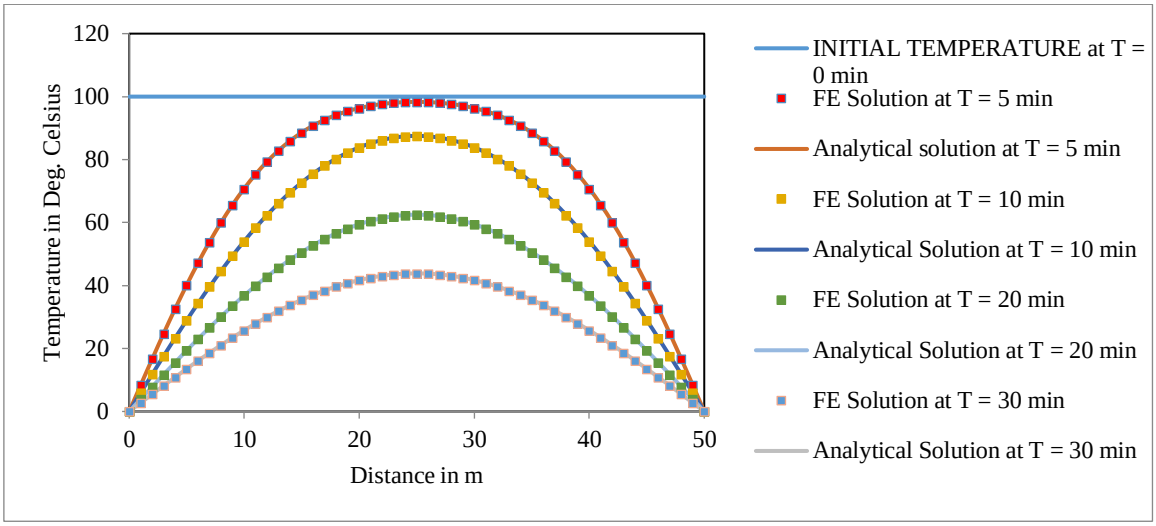

Fig. 2: Case A: Concentration profiles at any horizontal section parallel to the x-axis and at various times from time = 0 to time = 30 minutes (min)

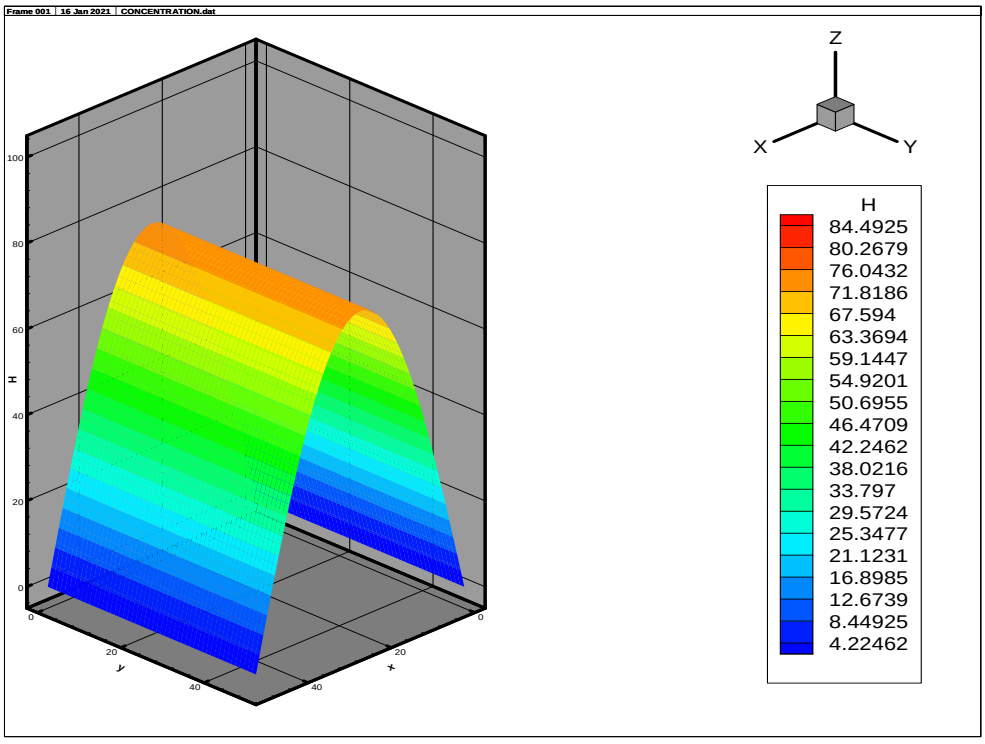

Fig. 3: Case A: Two-dimensional finite element concentration profile at time = 15 minutes showing disappearance of the initial horizontal plateau with pollutant escaping in the x-direction

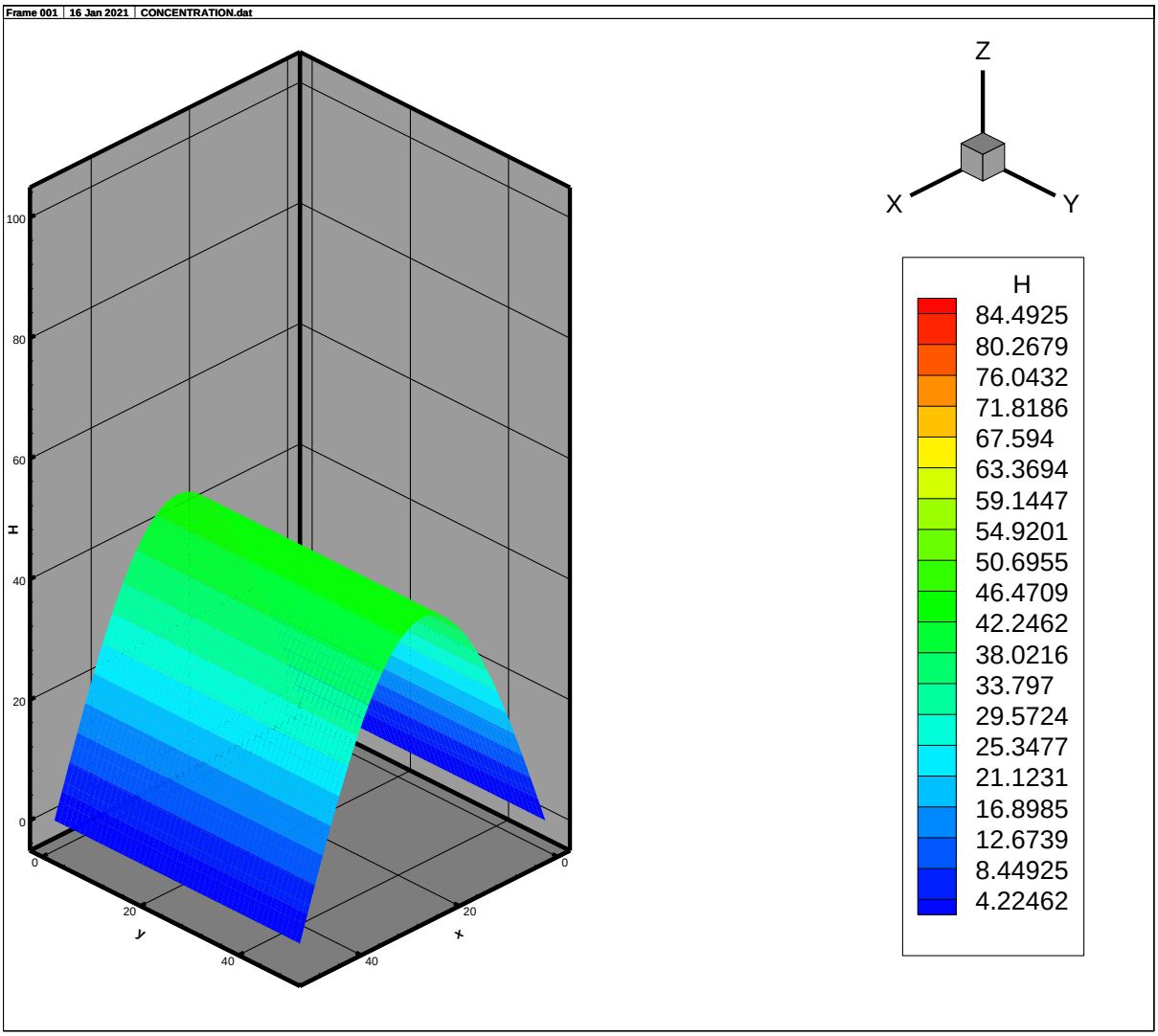

Fig. 4: Case A: Two dimensional finite element concentration profile at time = 30 minutes

Case B

For the diffusion process in the y direction, the transport equation becomes:

$$\frac{\partial c}{\partial t} = D_y \frac{\partial^2 c}{\partial y^2} \quad (6)$$

Now the boundary conditions are changed, opposite to the last case, such that $c = 0$ at $y = 0$ m and $y = 50$ m while $c_x = 0$ at $x = 0$ m and $x = 50$ m. The diffusion coefficient, D_y, is assumed equal to 0.15m^2/s, and the initial concentration distribution, c (x, y, 0), is assumed equal to 100 kg/m^3. The number of elements remained 2500. Figure (5) shows three Dimensional plot of the concentration profile at time = 1800s (30 minutes). In a way similar to the last case, the FE numerical and analytical solution profiles are in excellent agreement with a maximum difference of the percentage relative error of 0.07%. Similar to case A, the predicted concentration at the middle of the domain and at time of 30 minutes, i.e. c (25, 25 m, 1800s) was found to be 43.81926 kg/m^3, while the value given by the analytical solution is 43.84898 kg/m^3. It is concluded now that the two unsteady diffusion transport mechanisms in the x and y directions are working correctly, accurately, and stably.

Case C

Attention is now focused on dealing with the combined unsteady diffusion processes or transport mechanisms in the x and y directions as indicated by Eq. (2). The analytical solution is given by considering a rectangular 2D domain with length equal to L in the x-axis direction and height equal to H in the y-axis direction. The initial condition or data function is taken as c (x, y, 0) = C_o, and the following boundary conditions are considered:

DOI: 10.3844/ajessp.2025.89.109

$$c\,(0,y,t) = c\,(L,y,t)\,, c\,(x,0,t) = 0\; and\; c_y\,(x,H,t) = 0 \quad (7)$$

The analytical solution to Eq. (3) with the boundary conditions as given by Eq. (7) is given as:

$$c\,(x,y,t) = \sum_{m=1}^{\infty}\sum_{n=1}^{\infty} \frac{16\,C_o}{(2n-1)\,(2\,m-1)\pi^2} \sin\left(\frac{(2n-1)\,\pi\,x}{L}\right) \sin\left(\frac{(2m-1)\,\pi\,y}{2\,H}\right).\exp\left(-\left(\frac{(2m-1)^2}{4\,H^2}+\frac{(2n-1)^2}{L^2}\right)D\,\pi^2\,t\right) \quad (8)$$

Where D is the diffusion coefficient taken here as isotropic, i.e., $D_x = D_y = D$. To simplify matters and to compare with the previous cases (*A* and *B*) a square domain with side length equal to 50 m is considered, the diffusion coefficient *D* is assumed equal to 0.15 m /s, and C_o = 100 kg/m^3. A total of 100 terms were considered for the calculation of the Fourier series of the analytical solution in Eq. (8).

Figure 6 shows the concentrations at y = 50 m by the FE numerical model and the analytical solution in Eq. (8) where it can be seen that the corresponding values are in excellent match. Table 1 is the concentration at the point (25.0, 50.0) with a trend of nonlinear concentration decrease with time. After 1800s (30 minutes), the FE calculated concentration is 41.06485 kg/m 3 versus 41.09312 kg/m3 by the analytical solution. The maximum difference of the percentage relative error is 0.10676% which is still very good. Figures 7 to 14 show three and two-dimensional plots of the finite element model predictions of the concentration at different times, where the initial data function or horizontal plateau finally disappears. In all these figures, the smoothness of the finite element concentrations over the whole domain supports its power and strength in dealing with the two-dimensional unsteady diffusion transport mechanisms.

It is noted that Figures 7 to 14 depict the temporal evolution of pollutant dispersion under Case C conditions. The symmetry of the contour lines confirms numerical consistency with expected diffusion behavior. The progression of peak concentrations over time aligns with theoretical decay rates.

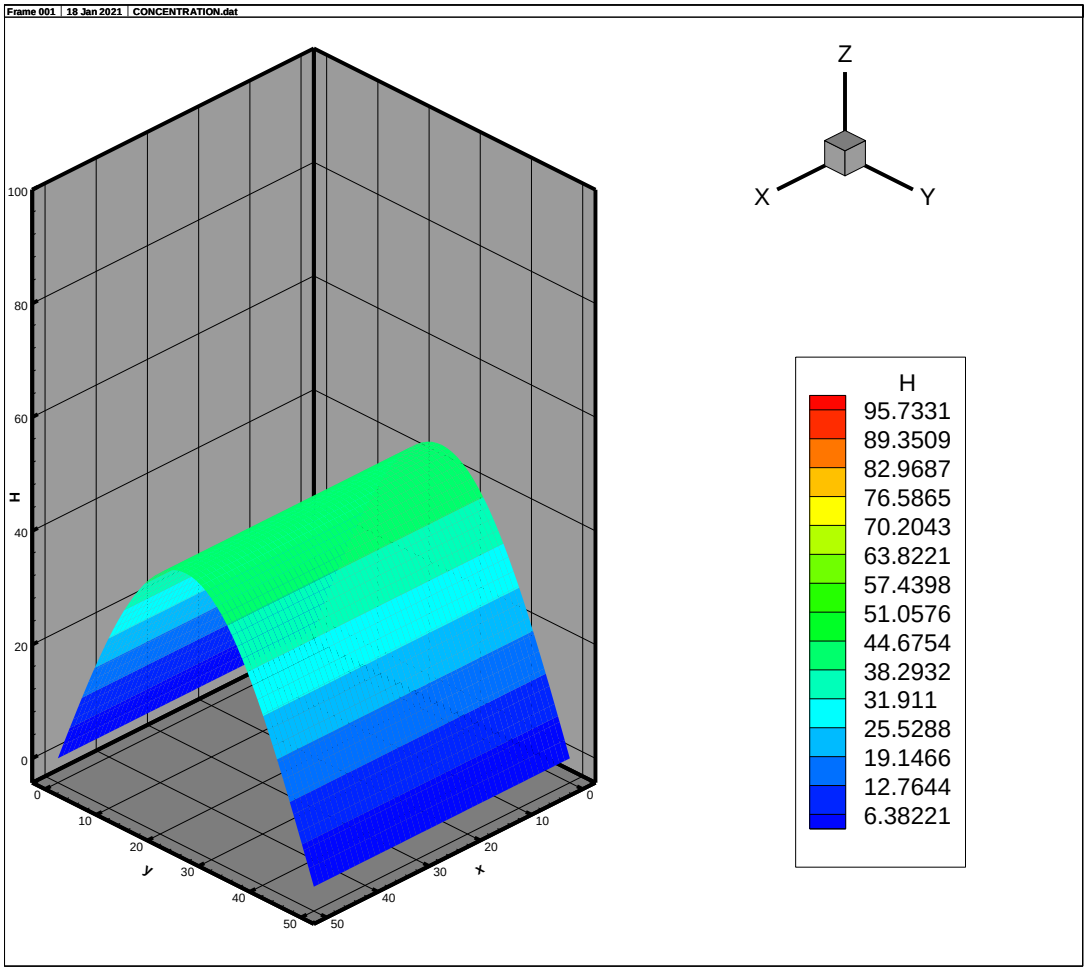

Fig. 5: Case B: Two-dimensional finite element concentration profile at time = 30 minutes; pollutant escapes in the y -y-direction

DOI: 10.3844/ajessp.2025.89.109

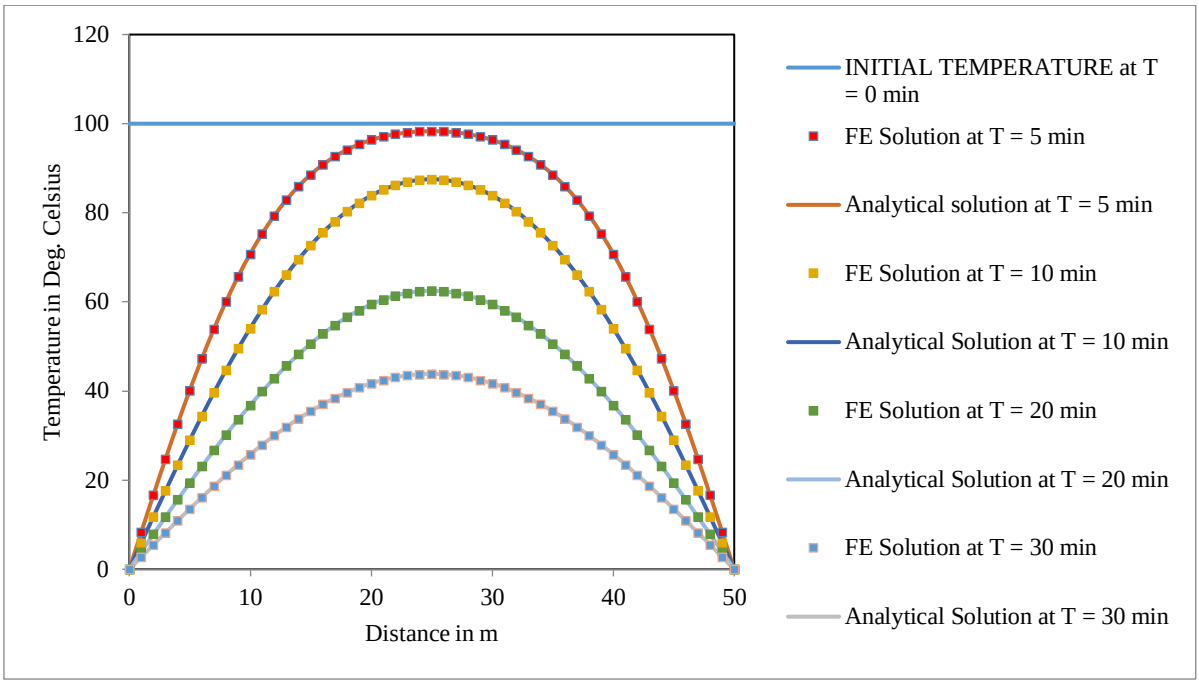

Fig. 6: Case C: Finite Element (FE) and analytical solutions for the concentration profiles at y = 50 m and at various times from time = 0 to time = 30 minutes; pollutant escapes in the x and y-directions

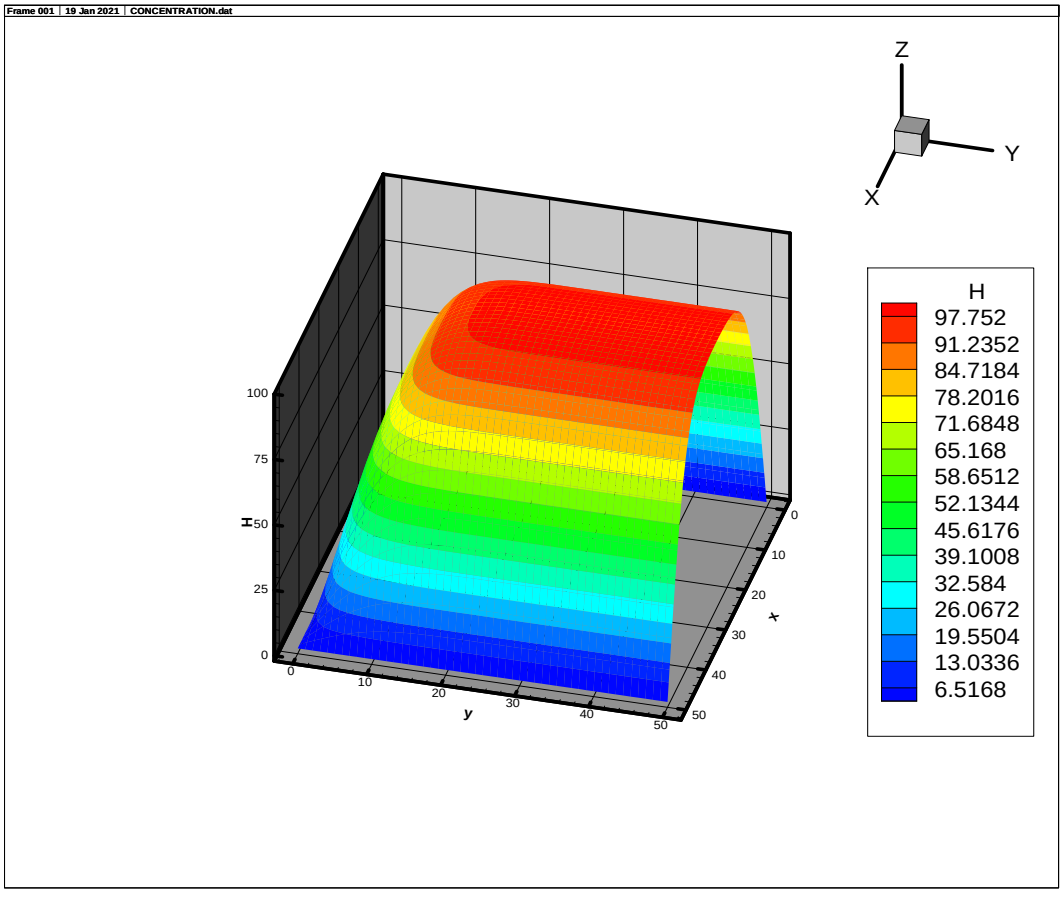

Fig. 7: Case C: Three-dimensional plot at time = 180s

DOI: 10.3844/ajessp.2025.89.109

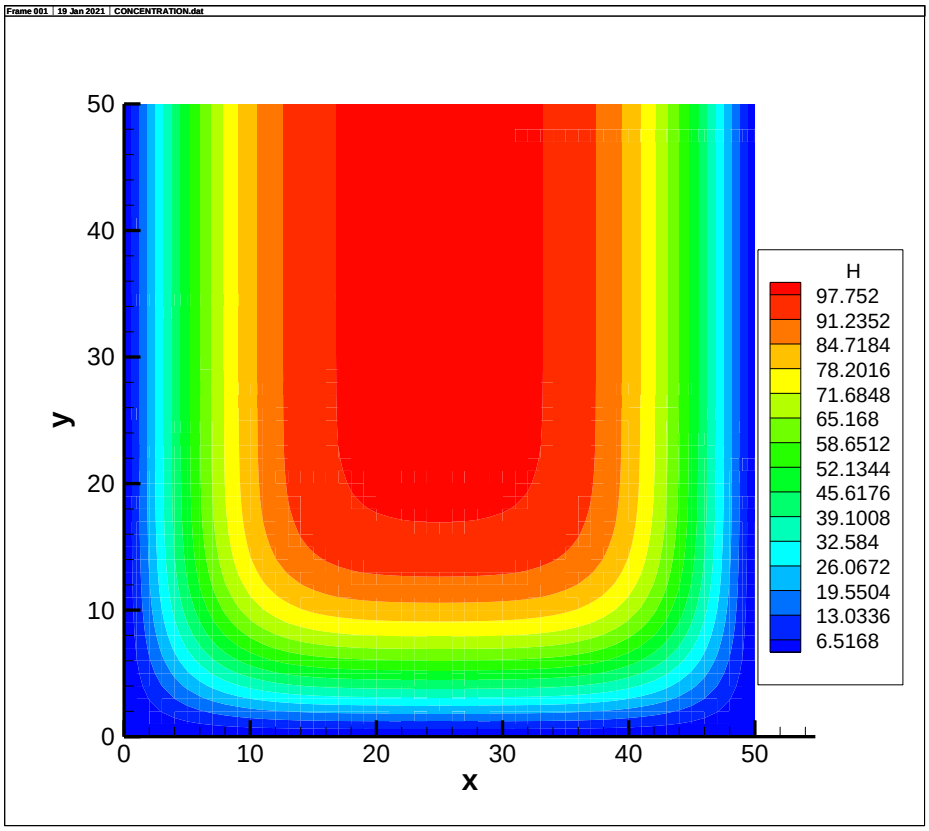

Fig. 8: Case C: Two-dimensional plot at time = 180s

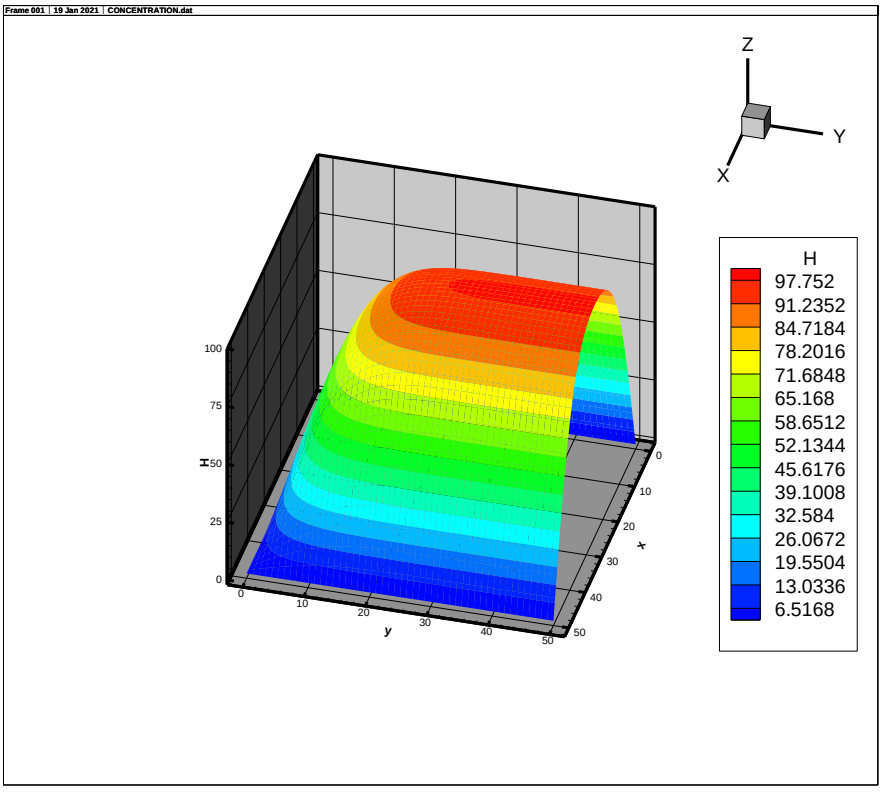

Fig. 9: Case C: Three-dimensional Plot at 300s

DOI: 10.3844/ajessp.2025.89.109

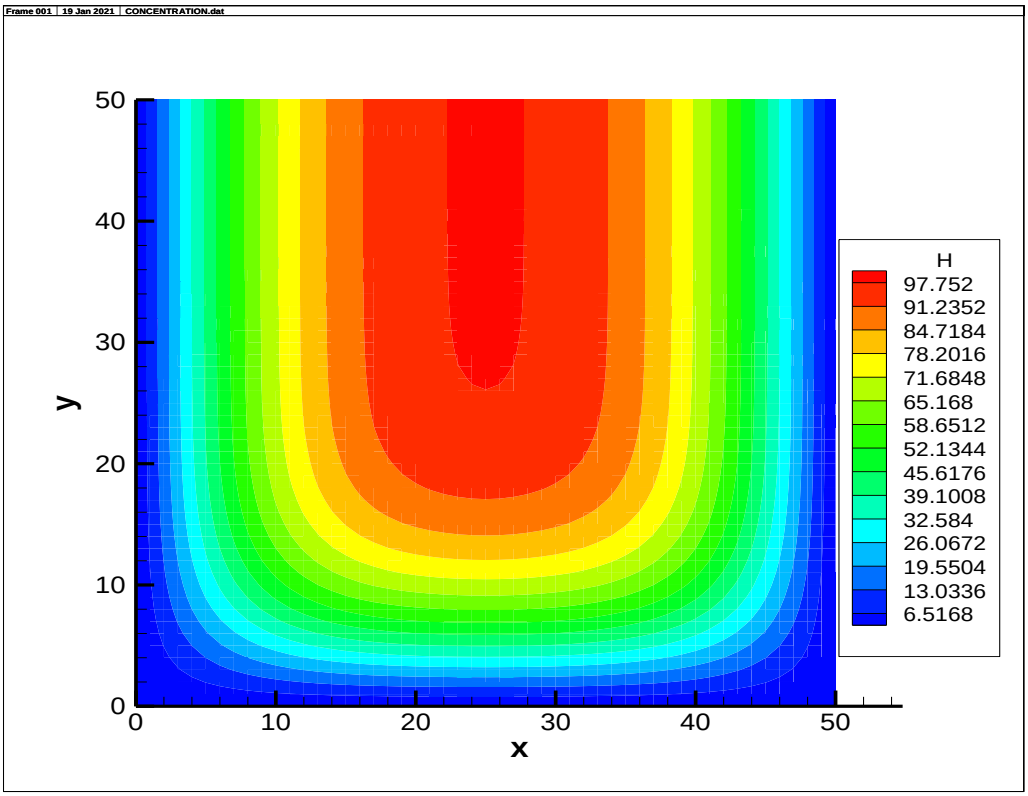

Fig. 10: Case C: Two-dimensional Plot at time 300s

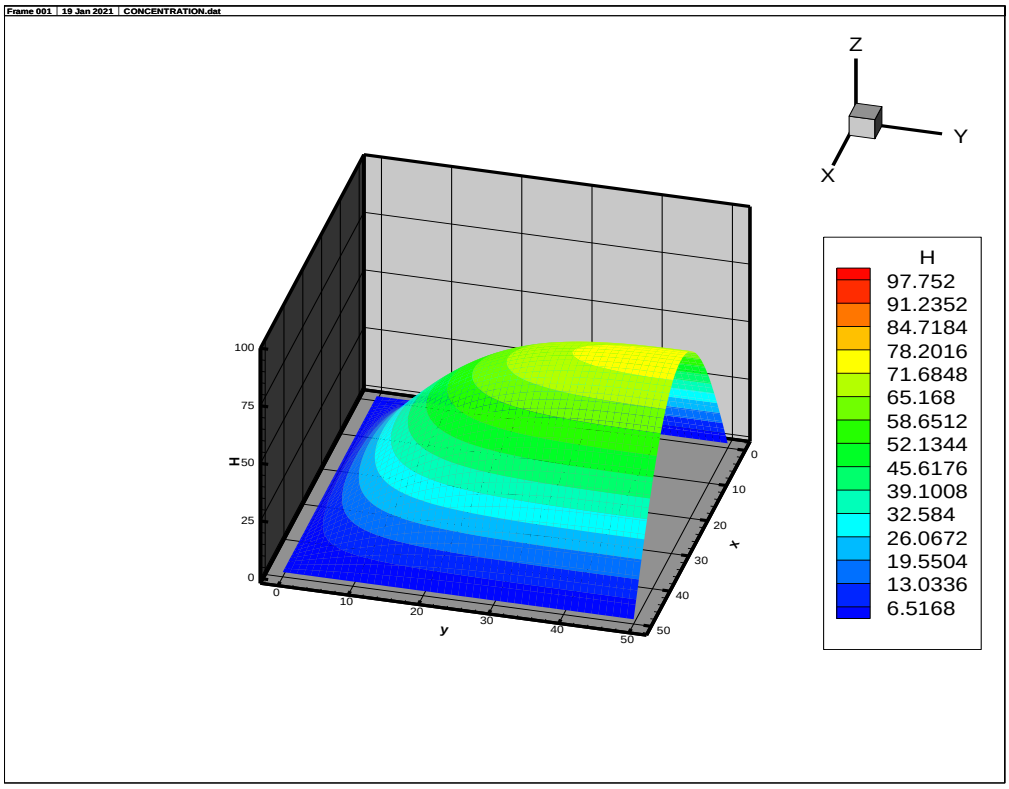

Fig. 11: Case C: Three-dimensional Plot at 900s

DOI: 10.3844/ajessp.2025.89.109

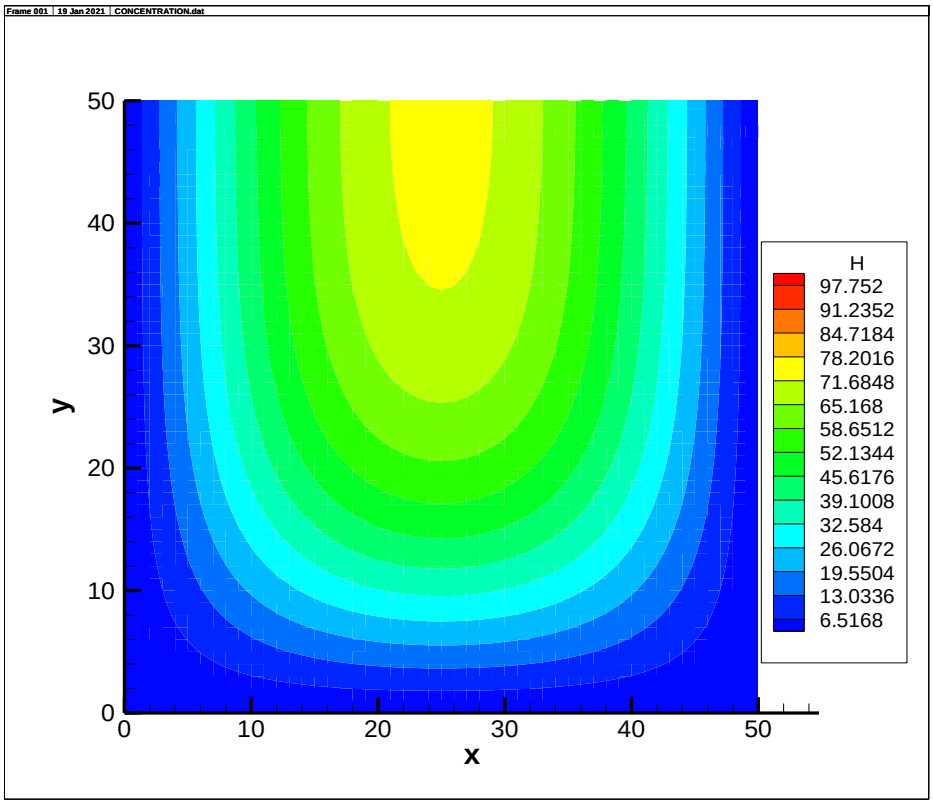

Fig. 12: Case C: Two-dimensional plot at time 900s

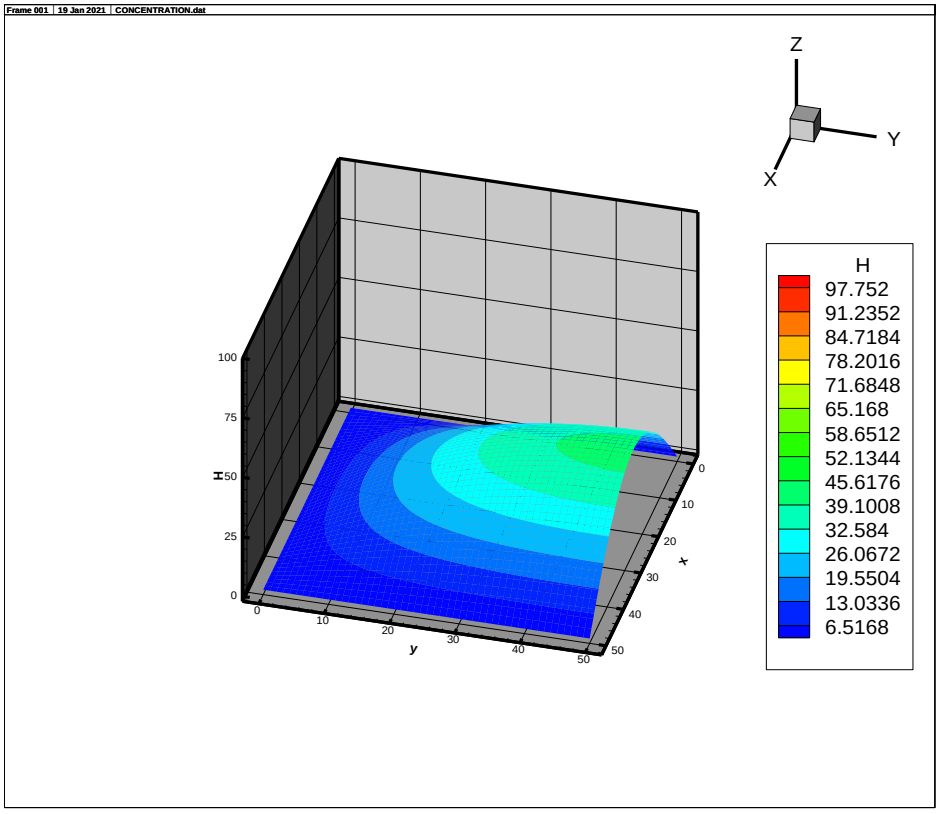

Fig. 13: Case C: Three-dimensional plot at 1800s

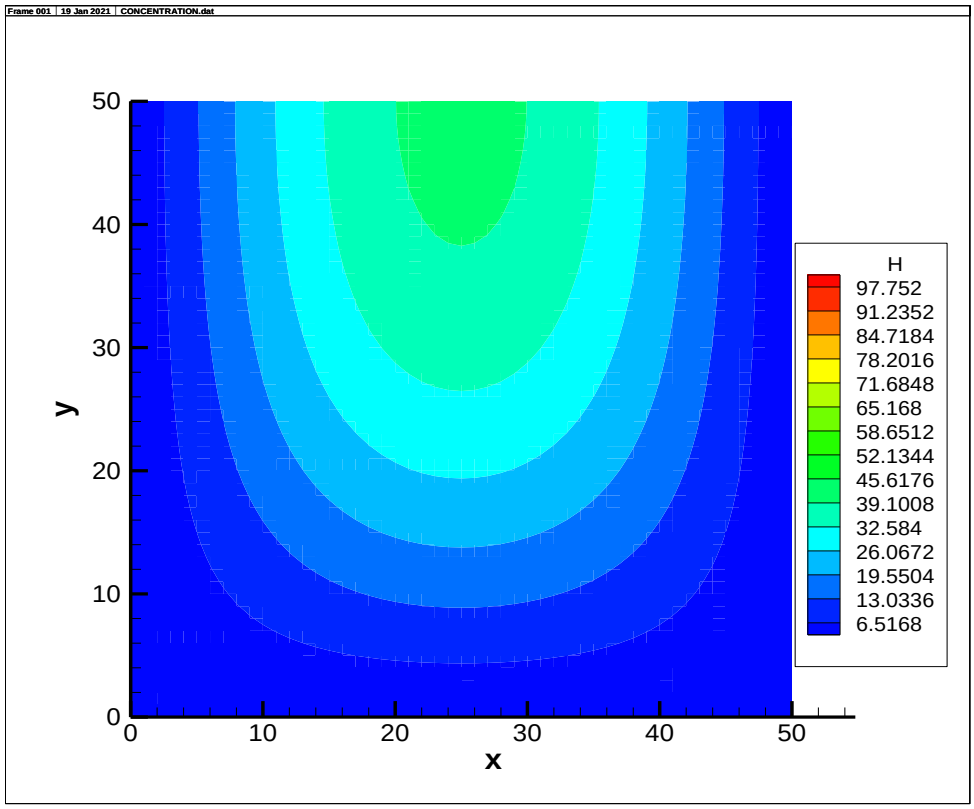

Fig. 14: Case C: Two-dimensional plot at time 1800s

Testing Advection and Diffusion Mechanisms

The advection and diffusion are the most important mechanisms or processes in the transport of substances such as pollutants when there is no decay and no generation. In the previous section, the diffusion mechanism was investigated successfully, and the FE numerical code proved its accuracy. In this section, attention is given to advection when combined with diffusion. The governing equation will be considered first in the *x*-axis direction and will be:

$$D_x \frac{\partial^2 c}{\partial x^2} - u \frac{\partial c}{\partial x} \quad (9)$$

Subjected to the following boundary conditions:

$$c(0, y, t) = 0,\ c(L, y, t) = C_L\ c_y(x, 0, t) = 0\ and\ c_y(x, H, t) = 0 \quad (10)$$

In the above boundary conditions, the domain is insulated at the two edges at $y = 0$ and $y = H$. As the FE numerical solution will be compared against the analytical solution, a small-sized domain would be sufficient. Therefore, 50 m in x direction with 200 divisions by 10 m in the y direction with 20 divisions would yield 4000 quadrilateral elements each element with 4-nodes. The FE code will run in unsteady mode (with time step equal to 0.5 s) until a steady state conditions occur and in that case the steady state analytical solution is given as:

$$c(x) = c_L \frac{(e^{(Pe)\,x} - 1)}{(e^{(Pe)\,L} - 1)} \quad (11)$$

Where C_L is the concentration at the boundary $x = L$ and L is the length of the domain in the x direction. C_L is assumed to be 10 kg/m3 while D_x and u will vary to produce different Peclet number values ($Pe = u\ L/\ D_x$), which control the mechanism of advection-diffusion. Values of the Peclet numbers are taken as 50, 5, and 1 representing: Very strong or nearly pure advection (Pe = 50), balanced advection and diffusion (Pe = 5), and finally strong diffusion or nearly pure diffusion (Pe = 1), respectively. Figure (15) shows for a longitudinal section along the x direction, excellent agreement between the FE numerical code and the analytical solution given by Eq. (11) in all three cases, even for the highly advective flow (Pe = 50) which is well known to constitute numerical convergence problems.

The highly or nearly pure advective flow at Pe = 50 pushes the boundary concentration further toward the other end. Figures 16 to 18 show Three Dimensional plot of the FE numerical code results, which illustrate further the profiles in Fig. (15). The case of Pe = 1 represents nearly pure diffusion, which has a nearly flat surface (linear cross-section profile). The maximum percentage relative errors between the FE code and the analytical solution are 0.0025, 0.76%, and 0.46%, for Peclet numbers 1, 5, and 50, respectively. For the 0.5s time step, it took nearly 1000 time steps to reach steady state conditions in all runs, which requires 2000 time steps.

DOI: 10.3844/ajessp.2025.89.109

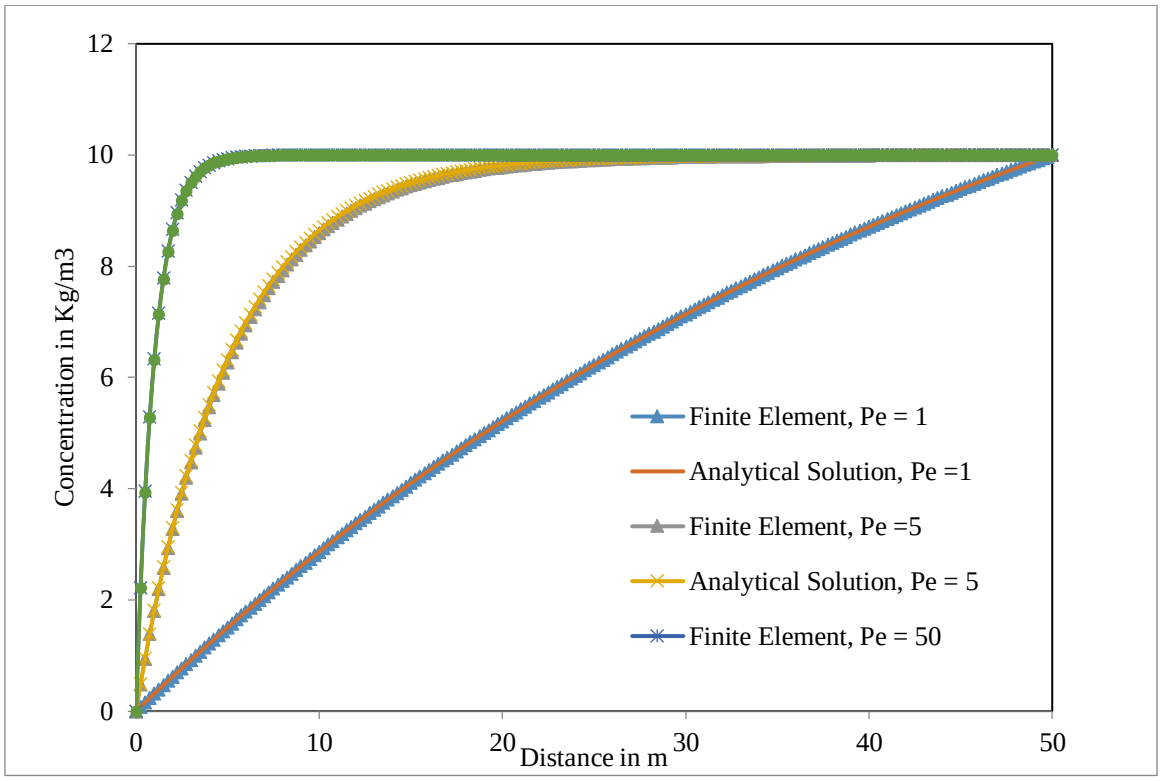

Fig. 15: Results for advection and diffusion-dominated flows for different Peclet numbers, Pe = u L/D_x

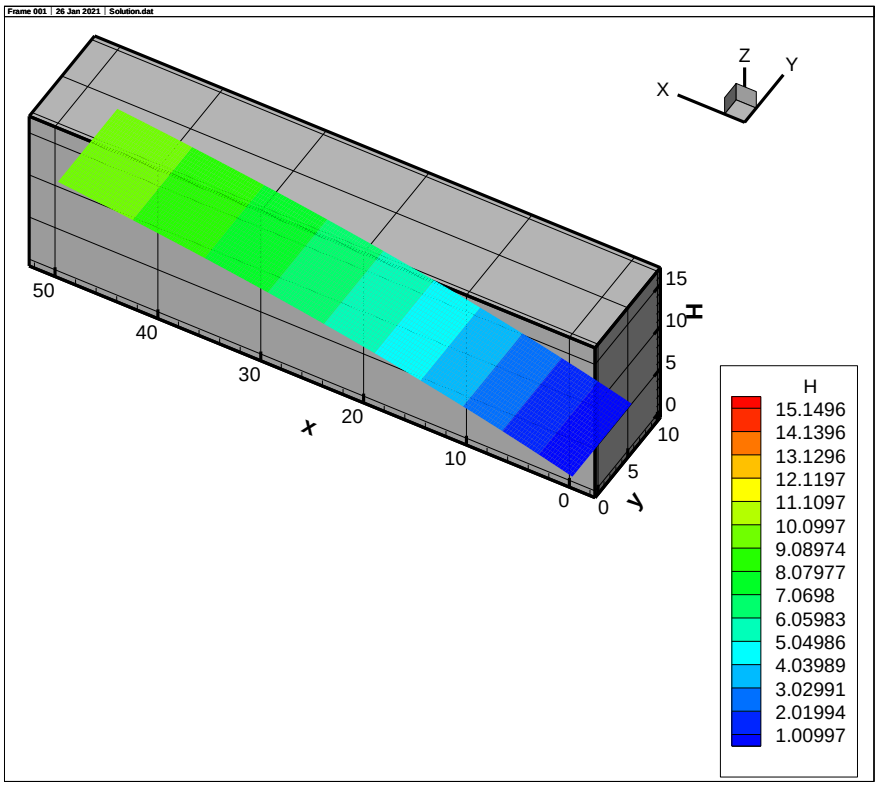

Fig. 16: Three-dimensional plot for advection and diffusion-dominated flows for Peclet number (Pe) = 1

DOI: 10.3844/ajessp.2025.89.109

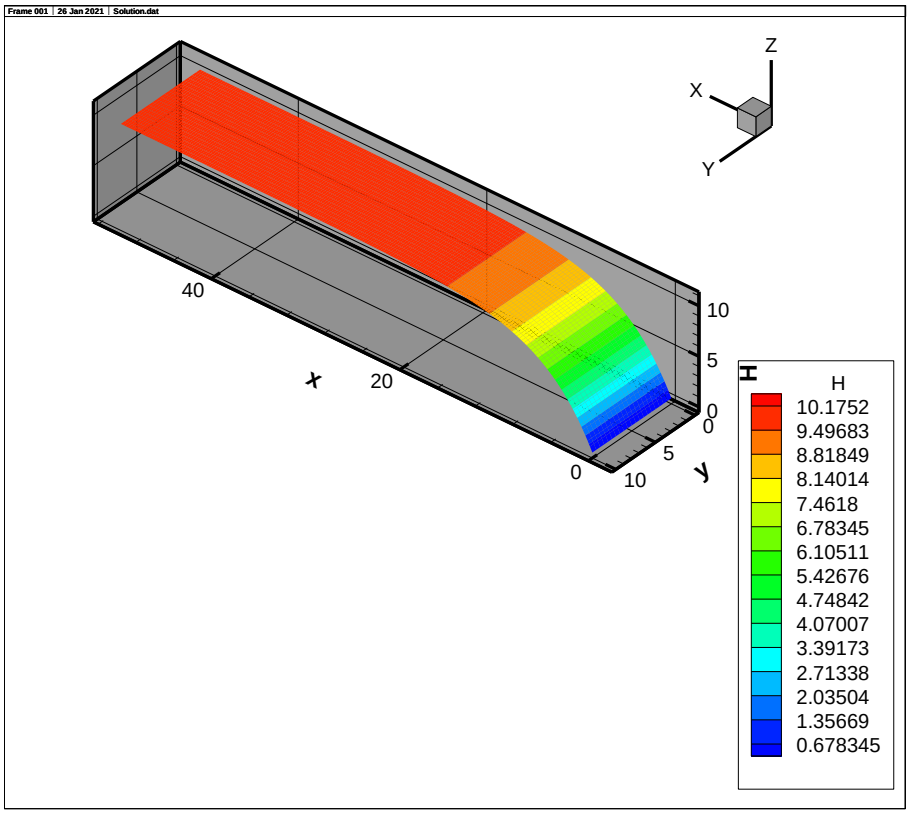

Fig. 17: Three dimensional plot for advection and diffusion-dominated flows for Peclet number (Pe) = 5

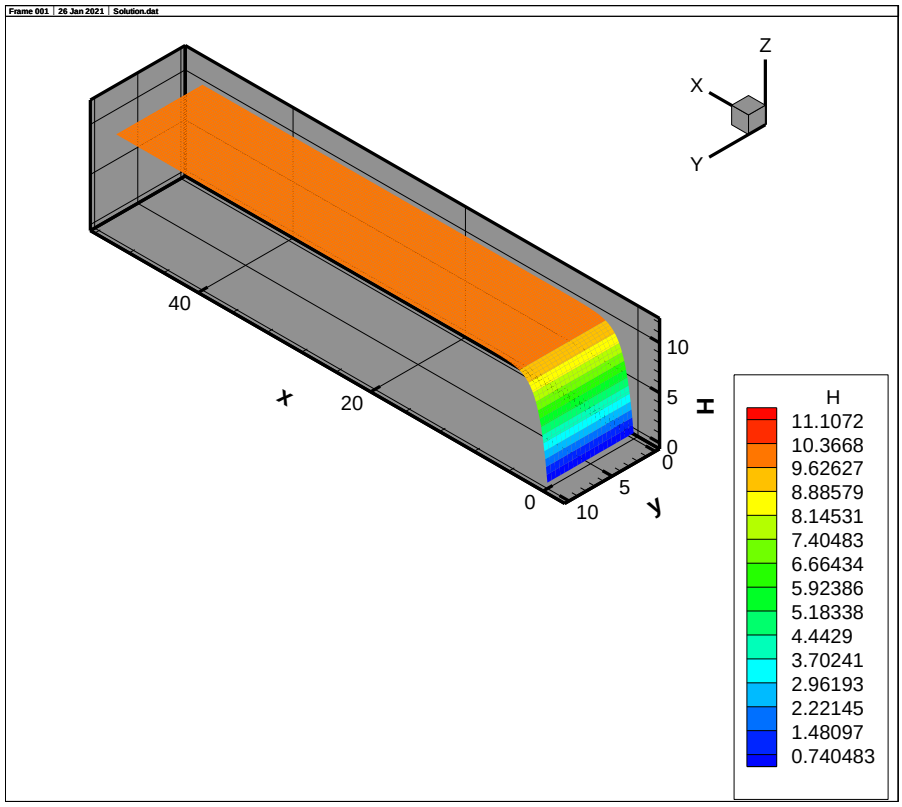

Fig. 18: Three dimensional plot for advection and diffusion dominated flows for Peclet number (Pe) = 50

DOI: 10.3844/ajessp.2025.89.109

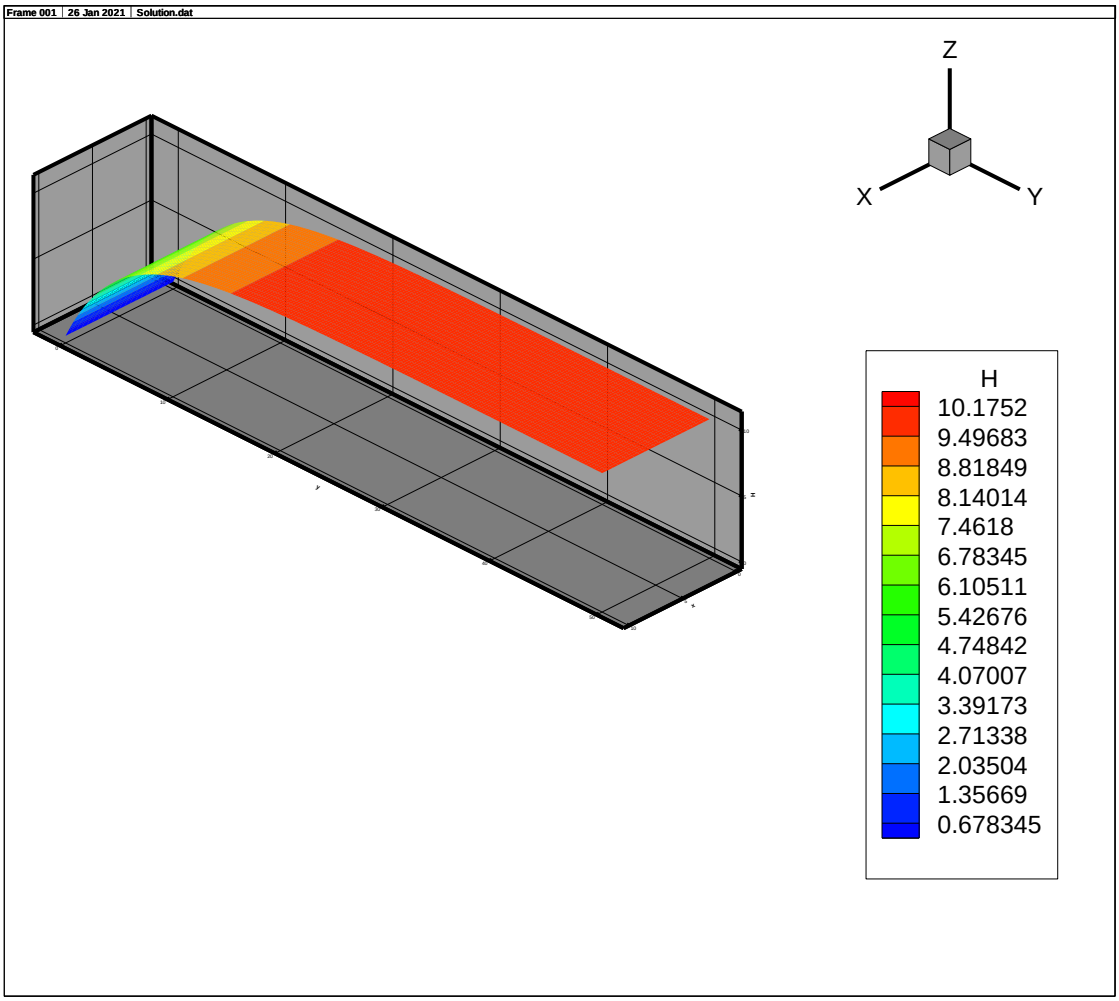

Fig. 19: Three-dimensional plot for advection and diffusion-dominated flows for Peclet number (Pe) = 10, where the flow is in the y direction

If the problem herein as represented by Eq. (9) and Eq. (10) along the x direction is rewritten along the y direction to test advection and diffusion in the y direction, the FE numerical code results are as in the Three Dimensional plot of Fig. (19). The maximum percentage relative error between the FE code and the analytical solution (written along the y direction) is 0.76% for P_e =5. In conclusion, the advection-diffusion mechanisms in both x and y directions are modelled accurately by the FE numerical code (SUITE-2D).

Testing Advection, Diffusion and Decay Mechanisms

The decay, advection, and diffusion mechanisms in the y direction can be represented in the following equation:

$$D_y \frac{\partial^2 c}{\partial y^2} - v \frac{\partial c}{\partial y} - k\, c = 0 \qquad (12)$$

The solution of Eq. (12), which has a steady state, is given by:

$$c(y) = c_L \exp\left(\frac{(L-y)v}{2D_y}\right) * \frac{\sinh\left(y\sqrt{\frac{v^2}{(4D_y{}^2)} + \frac{k}{D_y}}\right)}{\sinh\left(L\sqrt{\frac{v^2}{(4D_y{}^2)} + \frac{k}{D_y}}\right)} \qquad (13)$$

The model input parameters are such that C_L= 10 kg/m^3, L = 50 m, D_y = 0.5 m^2/s, v = 0.1 m/s, k = 0.2 1/s and the Peclet number is 10. Figure 20 shows that both the FE and analytical solutions are coincident. The maximum absolute difference in concentration is 0.00236 kg/m3, where the FE prediction is 3.88231 kg/m^3 while the analytical solution value is 3.88467 kg/m^3. Its location is close to the exit boundary at the point (0.5 m, 48.25m) with a corresponding percentage relative error of -0.06%. The decay effect is pronounced for the range of the parameters above. Figure 21 shows a Dimensional plot of the FE solution (SUITE-2D) in the y direction. The same trend is expected for the x-direction equation equivalent of Eq. (13).

DOI: 10.3844/ajessp.2025.89.109

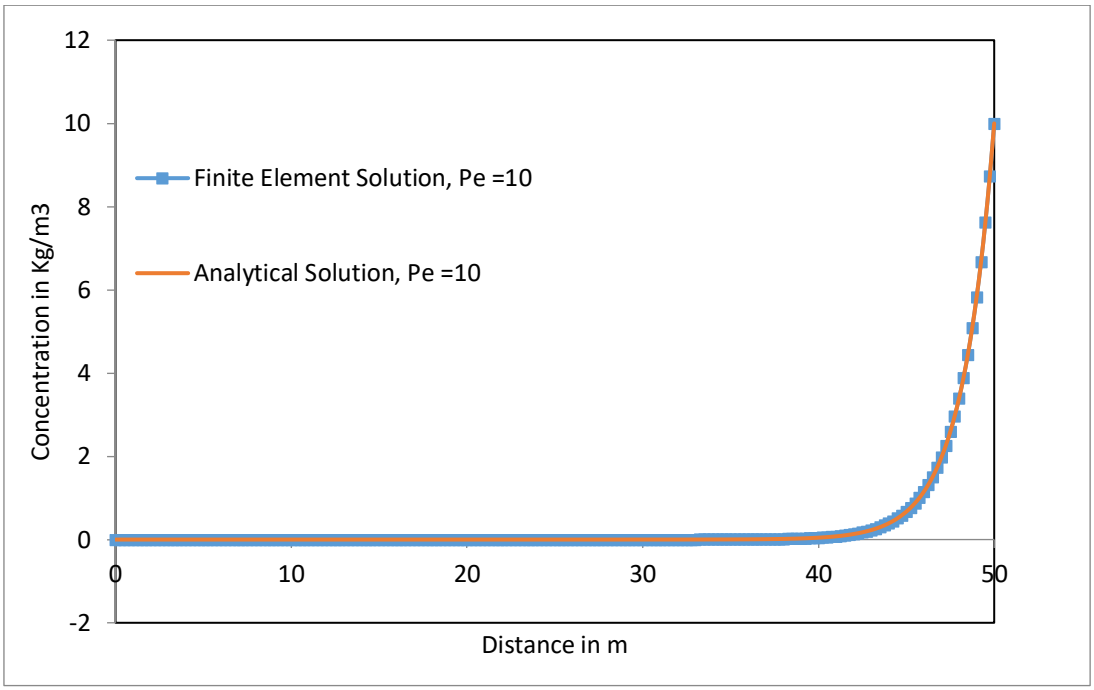

Fig. 20: FE and Analytical solutions for decay, advection and diffusion mechanisms for Pe = 10, T = 1000s

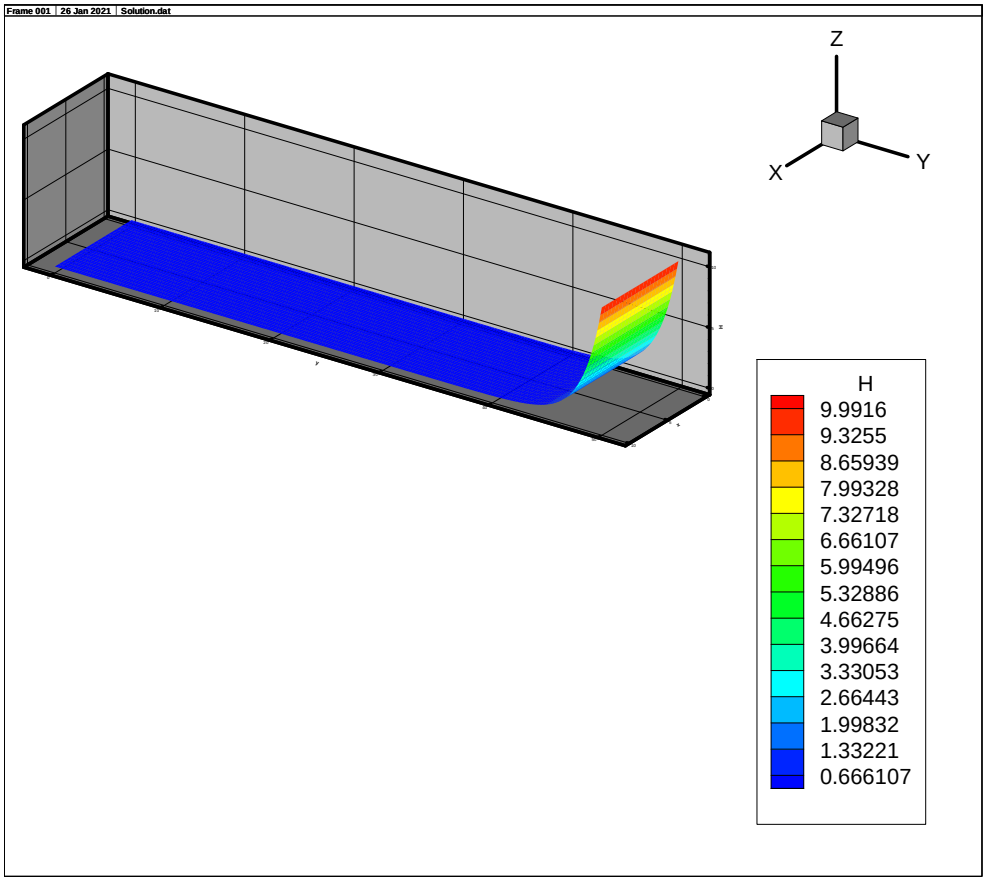

Fig. 21: Three-dimensional plot of the FE solution for decay, advection and diffusion mechanisms for Pe =10, T = 1000s

Demonstration of Advection and Diffusion Due to Pollution by an Industrial Point Source

After testing the diffusion, advection, and decay components in the developed FE numerical code (SUITE-2D) using existing analytical solutions, attention is now given to using this validated model for predicting the concentration of pollutants due to industrial sources. This means that the two-dimensional version of Eq. (1) is used. The case presented herein is discussed in Oyjinda and Pochai (2017) and is considered a demonstration, not a validation. This is primarily due to missing or ambiguous parameter values in the original source (Oyjinda and Pochai, 2017), no quantitative comparison could be conducted. The SUITE-2D results instead demonstrate plausible plume behavior under realistic input assumptions. A two dimensional vertical domain (x, z) of 1000 by 400 m is considered, where sulfur dioxide is released from a chimney with coordinates (100, 75) (m, m). The diffusion coefficients in the x- and z-directions are 2.0 and 0.45 m^2/s, while the wind velocities are assumed as 0.11 and $-6.9x10^{-3}$ m/s in the x- and z-directions, respectively. Oyjinda and Pochai (2017) used $\Delta x = \Delta z = 25$ m and a time interval of 72 s in their forward finite difference scheme. However, the lack of clarity in the reported value for the concentration of the point source pollutant prohibits direct quantitative comparison with the current model. In the current model, a load of 1.0 kg/s is assumed with a grid spacing of 25 m and a time step of 60 s. The current FE code uses central difference for treatment of the time derivative. Figures 22 to 25 show a 2D contour plot of the two two-dimensional concentrations at times of 30 minutes, 60 minutes, 90 minutes, and one day, respectively. It should be noted that Figures 22 to 25 illustrate a demonstration case inspired by Oyjinda and Pochai (2017). While exact parameters were unavailable, the results qualitatively match expected vertical dispersion trends. These are shown for illustrative purposes only.

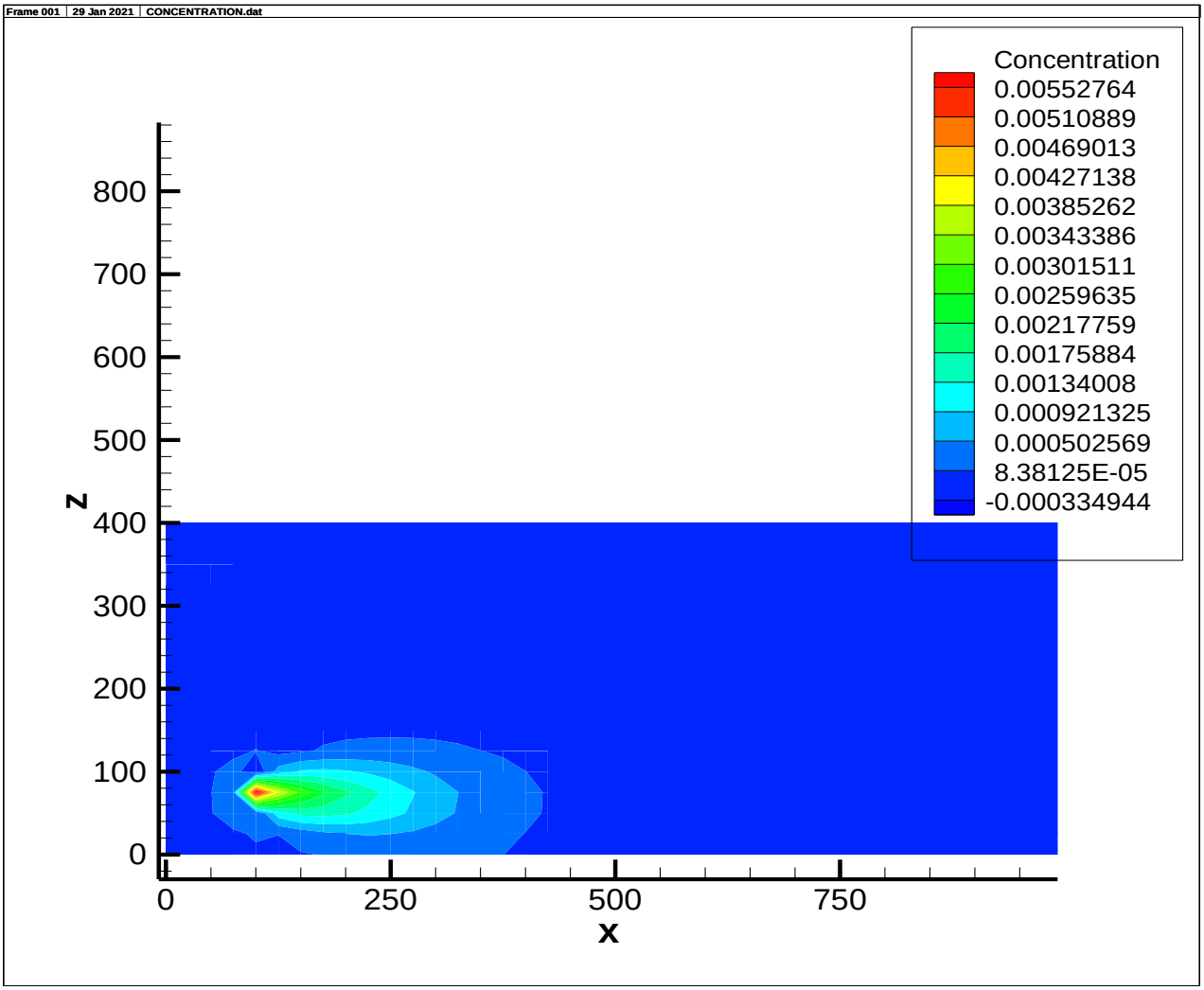

Fig. 22: Concentration profile due to point source pollutant at (100, 75 m) after 1800s (30 minutes)

DOI: 10.3844/ajessp.2025.89.109

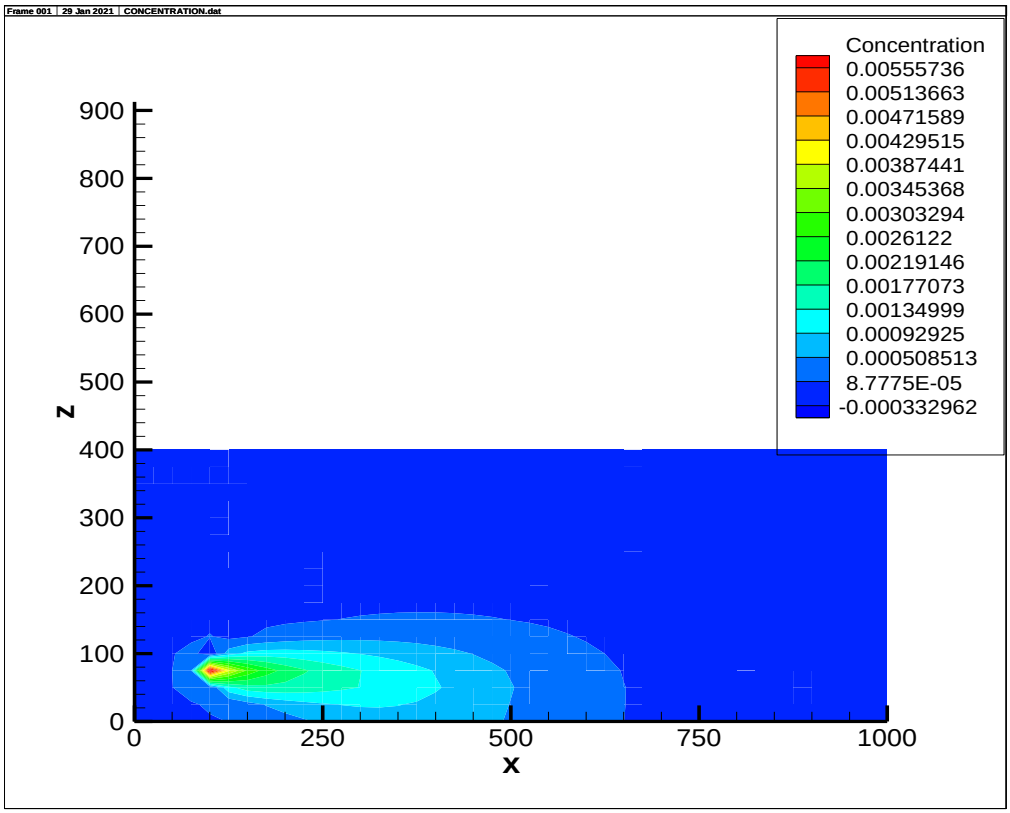

Fig. 23: Concentration profile due to point source pollutant at (100, 75m) after 3600s (60 minutes)

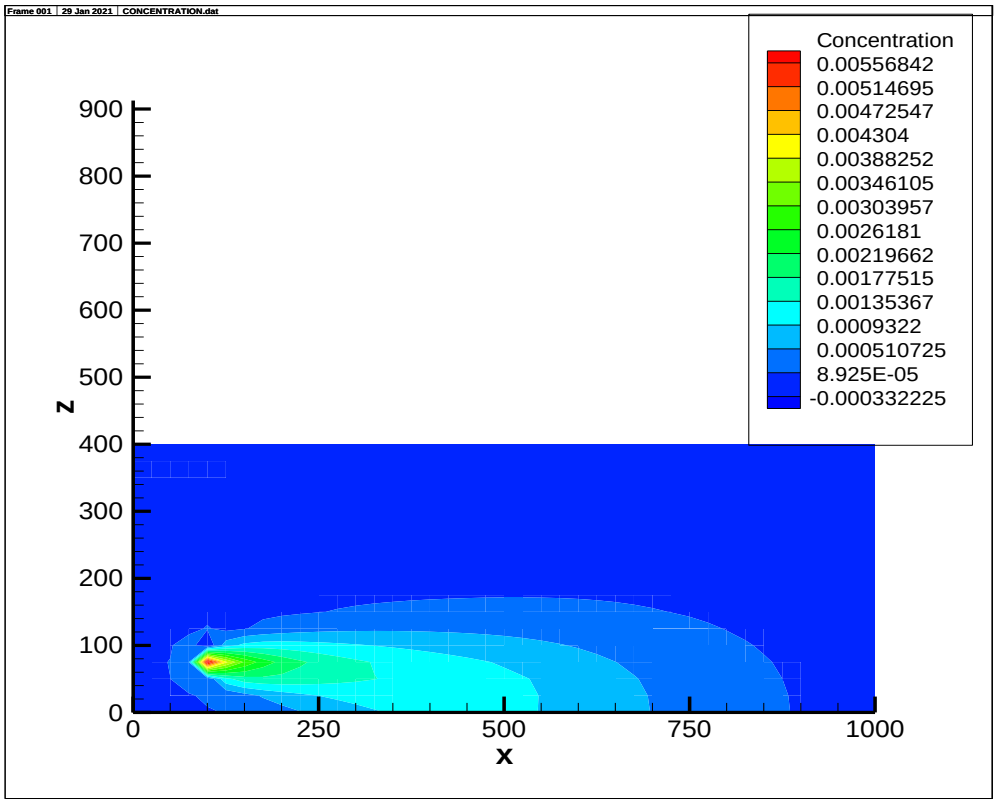

Fig. 24: Concentration profile due to point source pollutant at (100, 75 m) after 5400s (90 minutes)

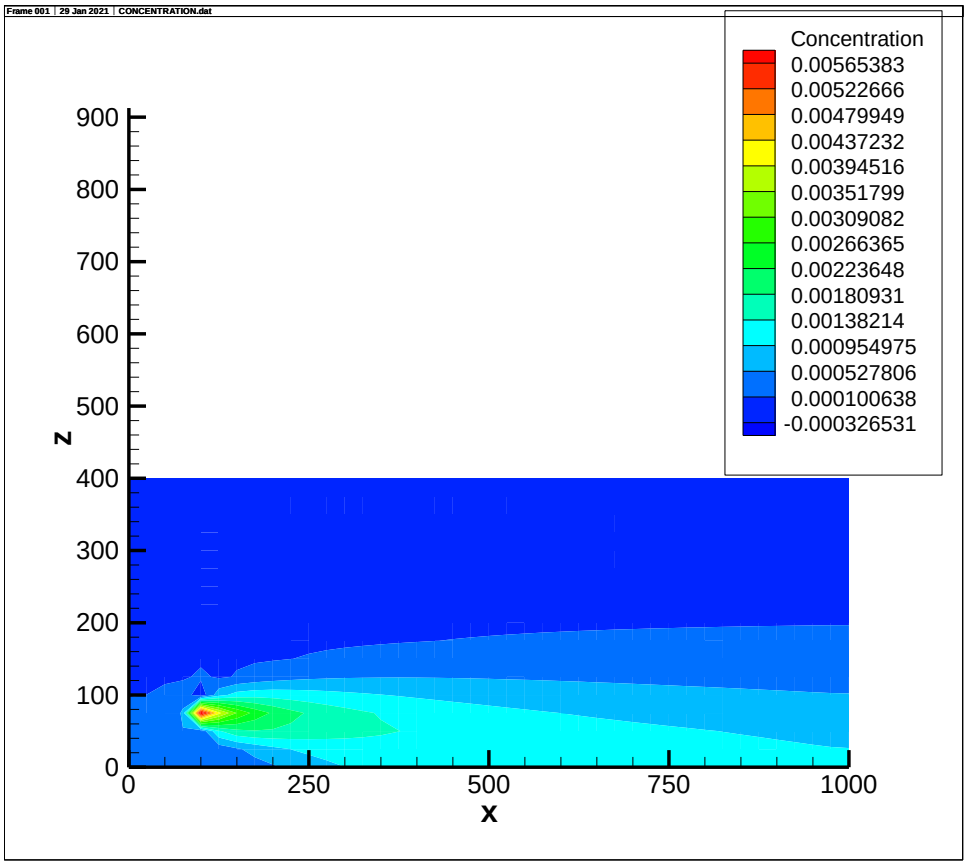

Fig. 25: Concentration profile due to point source pollutant at (100, 75m) after 86400s (1 day)

Discussion

The results obtained from the validation of SUITE-2D against exact analytical solutions demonstrate its accuracy and stability in modeling pollutant dispersion. The finite element approach adopted by the model ensures numerical robustness, even under complex transport conditions involving advection, diffusion, and decay mechanisms.

A key advantage of SUITE-2D is its computational efficiency compared to the previously developed SUITE-3D model (Hafez, 2022a). By reducing the dimensionality of the problem, SUITE-2D significantly lowers computational costs while maintaining reasonable accuracy for many practical applications. This makes it particularly suitable for scenarios where full 3D modeling may be unnecessary or computationally prohibitive.

Wind speeds and Peclet numbers (Pe = uL/D) were varied over a wide range (Pe = 1, 5, 10, 50) to represent diffusion-dominant, balanced, and advection-dominant regimes. The model is most reliable in domains with minor vertical variability (i.e., horizontally uniform conditions or in layers with known average properties). This study treats pollutant concentration generically to maintain generality across emission types. However, the model can be adapted to simulate specific pollutants (e.g., SO_2, NO_x, PM10) by assigning their decay coefficients, diffusivity, and reactivity properties, depending on atmospheric conditions or local emission standards such as those defined by the U.S. EPA or EEA.

However, the limitations of 2D modeling should be acknowledged. The assumption of uniformity in the third dimension may lead to inaccuracies in cases where vertical variations are significant, such as in highly stratified atmospheric conditions or near complex terrain. Future work could explore hybrid approaches that combine the computational efficiency of 2D modeling with selective 3D enhancements in critical regions.

The comparison between SUITE-2D and existing models for air pollution dispersion, including Gaussian plume models and puff-based models like CALPUFF, highlights the advantages of using a full differential equation-based approach. While Gaussian models offer rapid computations, they often oversimplify transport dynamics, particularly under low wind speed conditions. SUITE-2D, by contrast, captures the full range of transport mechanisms, providing more accurate and insightful predictions.

A clear comparison that differentiates SUITE-2D from SUITE-3D is that SUITE-2D reduces computational time by up to 90%, and that SUITE-2D typically runs 5–10 times faster than SUITE-3D for the same domain resolution. SUITE-2D reduces simulation time from hours to minutes, and memory usage by a similar factor and maintains solver architecture but simplifies geometry handling. SUITE-2D has applicability to horizontally homogeneous domains. This version of SUITE-2D assumes horizontally homogeneous flow and constant vertical profiles of temperature and wind. Therefore, limitations may arise under strong vertical wind shear or stratification. Future development will incorporate layered or 3D coupling to address such atmospheric complexities.

Conclusion

This paper presented the development and validation of SUITE-2D, a two-dimensional finite element model for solving the advection-diffusion transport equation with decay and source terms. The model's accuracy was confirmed through validation against exact analytical solutions, demonstrating its effectiveness in modeling pollutant dispersion in air systems.

Compared to the SUITE-3D model, SUITE-2D offers significant computational advantages while maintaining accuracy for a wide range of environmental applications. Its flexibility and robustness make it a valuable tool for environmental impact assessments and regulatory decision-making.

Future research directions include:

1. Extending SUITE-2D to incorporate dynamic boundary conditions and terrain effects
2. Developing a hybrid modeling approach that combines the computational efficiency of 2D modeling with selective 3D enhancements
3. Applying the model to real-world case studies involving complex industrial emission scenarios

By providing a reliable and efficient tool for modeling pollutant dispersion, SUITE-2D contributes to the advancement of environmental modeling practices and supports efforts to mitigate the impacts of industrial pollution.

Acknowledgment

The author acknowledges valuable feedback from AJES reviewers.

Funding Information

This research was self-funded.

Ethics

No human or animal subjects were involved. All data used are analytical or numerically generated.

References

Al-khafaji, F. M. A., & Al-Zubaidi, H. A. M. (2025). Numerical Modeling-Based Comparison of Leap-Frog and Implicit Crank-Nicolson Schemes for Instantaneous Spill of Pollutant in Rivers. *International Journal of Computational and Experimental Science and Engineering*, *11*(1). https://doi.org/10.22399/ijcesen.1190

Cheng, H., & Zheng, G. (2020). Analyzing 3D Advection-Diffusion Problems by Using the Improved Element-Free Galerkin Method. *Mathematical Problems in Engineering*, *2020*, 1–13. https://doi.org/10.1155/2020/4317538

Daly, A., & Zannetti, P. (2007). *Air Pollution Modeling: Theories, Computational Methods, and Available Software*.

Edwards, C.H. & Penney, D.E. (2009). Elementary Differential Equations with Boundary Value Problems (6th Edition, *Pearson International Edition*) pp. 137, 533-537.

Enciso-Díaz, W. C., Zafra-Mejía, C. A., & Hernández-Peña, Y. T. (2025). Global Trends in Air Pollution Modeling over Cities Under the Influence of Climate Variability: A Review. *Environments*, *12*(6), 177. https://doi.org/10.3390/environments12060177

Hafez, Y. I. (2022a). Understanding radon (222Rn) transport in one and multi-layer soils using analytical and finite element modeling. *Journal of Hydrology*, *610*, 127803. https://doi.org/10.1016/j.jhydrol.2022.127803

Hafez, Y. I. (2022b). Validated Three Dimensional Unsteady Finite Element Environmental Model, SUITE-3D, for Advection-Diffusion Flows and Air Pollution. *Journal of Engineering Science and Technology Review*, *15*(3), 139–146. https://doi.org/10.25103/jestr.153.12

Hafez, Y. I., & Awad, E.-S. (2016). Finite element modeling of radon distribution in natural soils of different geophysical regions. *Cogent Physics*, *3*(1), 1254859. https://doi.org/10.1080/23311940.2016.1254859

Issakhov, A., Alimbek, A., & Issakhov, A. (2020). A numerical study for the assessment of air pollutant dispersion with chemical reactions from a thermal power plant. *Engineering Applications of Computational Fluid Mechanics*, *14*(1), 1035–1061. https://doi.org/10.1080/19942060.2020.1800515

Jha, B. K., Adlakha, N., & Mehta, M. N. (2013). Two-dimensional finite element model to study calcium distribution in astrocytes in presence of excess buffer. *International Journal of Biomathematics*, *07*(03), 1450031. https://doi.org/10.1142/s1793524514500314

Leelossy, Á., Molnár, F., & Mészáros, R. (2014). Dispersion modeling of air pollutants in the atmosphere: A review. *Central European Journal of Geosciences*, *6*(3), 257–278. https://doi.org/10.2478/s13533-012-0188-6

Molinas, A., & Hafez, Y. I. (2000). Finite element surface model for flow around vertical wall abutments. *Journal of Fluids and Structures*, *14*(5), 711–733. https://doi.org/10.1006/jfls.2000.0295

Oyjinda, P., & Pochai, N. (2017). Numerical Simulation to Air Pollution Emission Control near an Industrial Zone. *Advances in Mathematical Physics*, *2017*, 1–7. https://doi.org/10.1155/2017/5287132

Putri, A. D., Rahardjo, I. S., & Nuryadi, R. (2018). Numerical simulation of BOD transport using finite difference methods in wastewater treatment plants. *Environmental Engineering and Management Journal*, *17*(4), 765–772. https://doi.org/10.30638/eemj.2018.078

Saqib, S., Akram, M., & Abbas, M. (2017). Efficient numerical schemes for solving three-dimensional advection diffusion equations using high order ADI methods. *Journal of Computational and Applied Mathematics*, *313*, 19–35. https://doi.org/10.1016/j.cam.2016.10.017

Sohrabi, Z., & Maleki, J. (2025). Fusing satellite imagery and ground-based observations for PM2.5 air pollution modeling in Iran using a deep learning approach. *Scientific Reports*, *15*(1), 21449. https://doi.org/10.1038/s41598-025-05332-2

Svoboda, T. D. (2000). Heat transfer through building constructions using finite element methods. *ASHRAE Transactions*, *106*(1), 458–467.

Talaa, A. M., Hafez, Y., Rashad, R. M., & Abdallh, E. (2002). Prediction of Heat and Mass Transfer Affecting Open Channels Environment. *Journal of Environmental Science, Ain Shams University*, *4*(3), 1110–0862.